

## Analytical Methods

## An aptasensor for ampicillin detection in milk by fluorescence resonance energy transfer between upconversion nanoparticles and Au nanoparticles

Chong Chen, Hong Lei, Nan Liu, Hui Yan\*

School of Biotechnology, Jiangsu University of Science and Technology, Zhenjiang 212100, China

## ARTICLE INFO

## Keywords:

Aptasensor  
Ampicillin  
Milk  
Upconversion  
Au nanoparticles  
Fluorescence resonance energy transfer

## ABSTRACT

This paper reports a portable fluorescence resonance energy transfer (FRET) aptasensor for ampicillin (Amp) detection using upconversion particles (UCNPs) as energy donors and Au nanoparticles (AuNPs) as energy acceptors. The optimal parameters of the detection system were investigated. Under the optimal conditions, it had a good linear relationship between the fluorescence intensities and Amp concentrations, a high coefficient of determination ( $R^2$ ) of 0.9939, a wide detection range of 10–100 ng/mL, and a low limit of detection (LOD) of 3.9 ng/mL; meanwhile, the aptasensor had high selectivity for Amp against the interference of other antibiotics, and had good recovery and repeatability. Also, its detection performance had been successfully validated by milk samples. Therefore, the developed aptasensor based on FRET between UCNPs and AuNPs has a good prospect for Amp on-site detection in milk with a portable upconversion detection instrument.

## 1. Introduction

Ampicillin (Amp) is a kind of  $\beta$ -lactam antibiotic, which inhibits bacterial transpeptidase to hinder the synthesis of the cell wall (Luo, Ang, & Thompson Jr, 1997). As a human and a veterinary drug, it has a strong bactericidal activity and a wide range of applications. However, Amp cannot be completely absorbed and metabolized, and a part of Amp remains in animal's body. It then can enter the human body through the food chain, which is harmful to human health. Partial Amp is excreted with feces and pollutes water sources and soil, through which it will be accumulated in food plants and will partially enter the human body (Elmolla & Chaudhuri, 2011).

Amp accumulation in the body will induce bacterial resistance and intestinal flora imbalance. In addition, Amp, as a hapten, can band tissue protein in the body to become a complete antigen, which will cause hypersensitivity reactions for a few special people (Abouzied, Sarzynski, Walsh, Wood, & Mozola, 2009). The European Union mandates the maximum residue limits (MRL) of Amp in milk and animal meat as 4  $\mu$ g/L and 50  $\mu$ g/L, respectively, and the Food and Drug Administration (FDA) stipulates Amp MRL in milk is 10  $\mu$ g/L (Song, Jeong, Jeon, Cho, & Ban, 2012).

Presently, several methods have been used for antibiotics detection in food, such as high-performance liquid chromatography (HPLC) (Luo, Ang, & Thompson Jr, 1997), enzyme-linked immunosorbent assay

(ELISA) (FitzGerald, O'Loan, McConnell, Benchikh, & Kane, 2007), and electrochemistry (Li, Zhu, Li, Liu, Li, & Kang, 2020), etc. However, expensive instruments and professional users are required to implement the analysis work, making them unable for a large number of detection tasks. Researchers have made great efforts to develop biosensors for portable and simple Amp detection. It has been documented that the gold-nanoparticles-based dual-fluorescence colorimetric aptamer sensor was developed for the trace detection of Amp in milk and water (Song, Jeong, Jeon, Cho, & Ban, 2012). A portable paper-based fluorescence immunoassay was reported for the trace detection of norfloxacin in milk (Zong, Jiao, Guo, Zhu, Gao, Han, et al., 2019). A colorimetric-based point-of-care testing method, in which the fluorescence image of the sample was obtained through a smartphone camera, was developed for streptomycin detection in milk, it had the advantages of good selectivity, simple operation, and on-site detection (Lin, Yu, Cao, Guo, Zhu, Dai, et al., 2018). A fluorescent-internal-filter-based test strip was designed for the rapid on-site visual detection of tetracycline, it has the advantages of simple operation and easy portability (Gan, Hu, Xu, Zhang, Zou, Shi, et al., 2021). Although the above portable detection methods did not require expensive instruments, they all used traditional fluorescent dyes, which were often excited by ultraviolet light and can induce sample autofluorescence, therefore, false positives were easy to occur.

UCNPs have anti-Stokes luminescence properties, and can absorb long-wavelength low-energy light and emit short-wavelength high-

\* Corresponding author at: School of Biotechnology, Jiangsu University of Science and Technology, Zhenjiang 212018, Jiangsu, China.

E-mail address: [yan\\_hui@just.edu.cn](mailto:yan_hui@just.edu.cn) (H. Yan).

energy light (Guo, Xie, Huang, & Huang, 2016; Xu, Chen, & Song, 2017). Because the long-wavelength light is weakly absorbed by biological samples, it can avoid the interference of sample autofluorescence. Accordingly, UCNP are better than traditional down-conversion fluorescent dyes (Wu, Duan, Ma, Xia, Wang, Wang, et al., 2012) for the complex samples matrixes, such as foods and biomedical samples (Gao, Zheng, Liu, Han, Li, Luo, et al., 2021; Li, Wang, Huang, & Chen, 2019; Yang, Li, Wu, Zhang, Feng, Yu, et al., 2021). Due to its high Stokes shift, narrow emission band, high photostability, and low autofluorescence (Long, Li, Zhang, & Yao, 2015), UCNP, in this study, were used as the fluorescent probe for Amp detection. In addition, a portable upconversion fluorescence instrument was applied, it had the advantages of small size, low weight, and simple operation (Xu, Chen, & Song, 2017), compared to the traditional upconversion measurement instruments based on photomultiplier tubes and monochromators.

FRET is a mechanism that describes the transfer of energy between two light-sensitive molecules (chromophores) (Cheng, 2006). The donor chromophore, which is initially in an electronically excited state, can transfer energy to the acceptor chromophore through nonradiative dipole-dipole coupling (Helms, 2008). The generation of FRET needs to meet two conditions: one is that the spatial distance between the donor and the acceptor is less than 10 nm, and the other is the overlap between the emission spectrum of the energy donor and the absorption spectrum of the acceptor (Wang, Hou, Mi, Wang, Xu, Teng, et al., 2009). Herein, we established a label-free aptamer sensor system based on FRET (UCNPs and AuNPs) for the simple, immediate, and sensitive detection of Amp. The detection principle is shown in Scheme 1. It consisted of UCNP, AuNPs, Amp aptamer (Apt), Amp, and NaCl, UCNP were used as energy donors, while AuNPs were as acceptors. When they were mixed, positively charged UCNP and negatively charged AuNPs approached each other through electrostatic adsorption, which led to the fluorescence quenching of UCNP by FRET. When NaCl was introduced, NaCl solution shielded the charges on the surface of AuNPs, consequently, AuNPs stayed away from UCNP and formed aggregation, and then the fluorescence of UCNP was restored. However, when Apt was introduced into the system, it was strongly adsorbed on the surface of AuNPs through the coordination between nitrogen atoms (in Apt) and AuNPs, therefore, the phosphoric skeleton of Apt covered the surface of AuNPs, and the electrostatic repulsion prevented from their aggregation, which enhanced the stability of AuNPs in a salt solution

and led to the fluorescence quenching of UCNP. In the measurement, when Amp was added to the system, Apt would preferentially combine with Amp. With the increase of Amp concentration, AuNPs absorbing Apt decreased, resulting in AuNPs aggregation, which led to the decrease of the fluorescence quenching effect of AuNPs on UCNP, therefore, the fluorescence intensity of UCNP was restored. It had a linear relationship between Amp concentration and UCNP fluorescence intensity, therefore, Amp concentration could be measured.

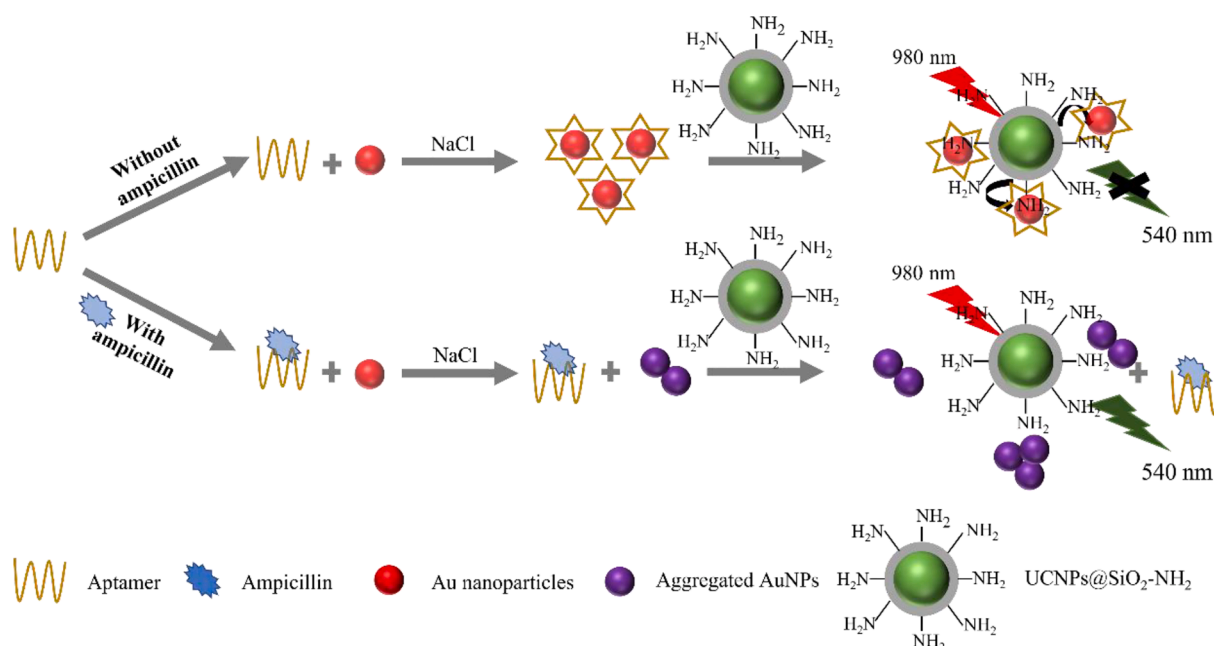
## 2. Materials and methods

### 2.1. Materials

Yttrium (III) chloride hexahydrate ( $\text{YCl}_3 \cdot 6\text{H}_2\text{O}$ , 99.99 %), Ytterbium (III) chloride hexahydrate ( $\text{YbCl}_3 \cdot 6\text{H}_2\text{O}$ , 99.99 %), and Erbium (III) chloride hexahydrate ( $\text{ErCl}_3 \cdot 6\text{H}_2\text{O}$ , 99.99 %) were purchased from Shanghai Aladdin Biochemical Technology Co., Ltd. (Shanghai, China). Oleic acid (90 %) and 1-Octadecene sodium (90 %) were purchased from Shanghai Aladdin Biochemical Technology Co., Ltd. (Shanghai, China). Chloroauric acid tetrahydrate ( $\text{HAuCl}_4$ , 99.9 %) and tetraethoxysilane (TEOS) were supplied by Sinopharm Chemical Reagent Co., Ltd. (Shanghai, China). Igepal CO-520 was purchased from Rhawn Chemical Technology Co., Ltd (Shanghai, China). Apt 5'-GCGGC GGTG TATAG CCG-3' was synthesized by Sangon Biotech (Shanghai) Co., Ltd. (Shanghai, China). All unspecified reagents were of analytical reagent grade and millipore milli-Q ultrapure water was used in this study.

### 2.2. Apparatus

Transmission electron microscope (TEM) images were taken using a HT-7800 electron microscope (Hitachi, Ltd, Tokyo, Japan, Japan). The absorption spectra of AuNPs under different conditions were recorded by a USB 4000 spectrometer (Ocean Optics, Orlando, FL., USA). The fluorescence emission spectra of UCNP were performed using a XS11639 spectrometer with a 980 nm excitation laser and FPB-980-1.5-FS-1B probe (Shanghai Ruhai photoelectric technology Co., Ltd., Shanghai, China).



**Scheme 1.** The principle of the aptasensor for Amp detection.

### 2.3. Synthesis and surface modification of UCNPs

UCNPs were synthesized according to the references with a little modification (Liu, Ouyang, Li, Zhang, & Chen, 2017). 1.0 mmol rare earth chloride (Y: Yb: Er = 78:20:2) was added to a 250 mL three-neck round-bottom flask containing 6 mL oleic acid (OA) and 15 mL 1-octadecene (ODE), mixed under magnetic stirring. Then, high-purity nitrogen gas was passed through for 10 min to exhaust the air in the flask. Under the protection of high-purity nitrogen gas and magnetic stirring, heat up to 160 °C and hold for 30 min to form a uniform solution. Subsequently, the temperature was dropped to 50 °C, and a 10 mL methanol solution containing 2.5 mM NaOH and 4 mM NH<sub>4</sub>F was slowly added to the solution, and maintained for 30 min to remove methanol from the solution. Raised the temperature to 70 °C and maintained it for 15 min for further removing methanol. It was then heated to 100 °C and maintained for 10 min to remove air. The temperature was continued to rise to 300 °C and maintained for 1 h to form UCNPs. The solution was naturally cooled to room temperature. Finally, UCNPs were collected by centrifugation at 8000 rpm for 8 min and were washed three times with ethanol cyclohexane (v: v = 1:1) solution and were dried in a vacuum oven at 60 °C.

In order to obtain water soluble UCNPs, a layer of aminated silica was coated by the following procedure (Jalil & Zhang, 2008). Firstly, 8.0 mg UCNPs powder was added to a flask containing 4 mL cyclohexane and sonicated for 5 min to fully disperse. Secondly, a mixture of 0.1 mL Igepal CO-520 and 6.0 mL cyclohexane was added and stirred for 10 min. Subsequently, 400 µL CO-520 and 80 µL 30 % (wt./v) ammonia water were continually added to the flask with stirring. The flask was sealed and sonicated for 20 min to form a homogeneous solution. Then 40 µL TEOS was slowly added and stirred at high speed for 11 h. Finally, 15 µL APTES was added and continually stirred for 1 h to form UCNPs@SiO<sub>2</sub>-NH<sub>2</sub>.

### 2.4. Synthesis of AuNPs

AuNPs with a average diameter of 13 nm were prepared (supplementary material) according to the referenced method (Shi, Zhao, Liu, Fan, & Cao, 2013). According to Beer's law, the concentration of AuNPs was about 9.6 nM (Haiss, Thanh, Aveyard, & Fernig, 2007).

### 2.5. Analysis method construction for Amp detection

In this work, the method of Amp detection was designed as follows: 56 µL Amp with different concentrations was added to 62 µL 0.4 µM Apt solution and was mixed with vortex oscillation, and incubated for 10 min. Then, 266 µL 4.8 nM AuNPs solution was successively added and then reacted for another 8 min. Subsequently, 266 µL 90 mM NaCl was added and thoroughly shaken for 13 min. Finally, 100 µL 0.1 mg/mL UCNPs@SiO<sub>2</sub>-NH<sub>2</sub> was quickly added. After vortex mixing, recorded the fluorescence spectra in the wavelength range 400–700 nm under the excitation of a 980 nm laser. In order to obtain a high performance system for Amp detection, several important parameters, including the concentrations of NaCl and Apt, and the reaction time of NaCl-AuNPs, Apt-AuNPs, and Apt-Amp, were investigated.

### 2.6. Real sample detection

To validate the feasibility of this method, milk samples purchased from local supermarkets were tested. The samples were pretreated according to the national standard method (NY/T 829–2004, China). 4 mL milk was added to 20.0 mL 75 % acetonitrile, oscillated by vortex for 5 min, and then centrifuged at 8000 r/min for 10 min to remove the proteins in milk, and the supernatant was passed through a 0.22 µM membrane to remove the lipids. Subsequently, the detection was carried out with the developed method in section 2.5 and the reference method (HPLC), respectively. Three spiked samples were tested, and three

parallel measurements were performed for each sample.

## 3. Results and discussion

### 3.1. Characterization of UCNPs and AuNPs

The morphology of UCNPs TEM is shown in Figure s1 (supplementary material). They were hexagonal with uniform particle size distribution and an average particle size of 55 nm. The size of UCNPs@SiO<sub>2</sub>-NH<sub>2</sub> was increased to 70 nm by coating SiO<sub>2</sub> on UCNPs, therefore, the thickness of the SiO<sub>2</sub> layer was 7.5 nm.

AuNPs were synthesized by the sodium citrate reduction method, and the size was affected by the amount of sodium citrate in the synthesis process (Frens, 1973). AuNPs were characterized by UV–vis spectroscopy and TEM. As shown in Fig. s2A, its absorption peak was at 520 nm, which was consistent with the literature (Chen, Sheng, Wang, Ouyang, Wang, Ali, et al., 2020). The TEM photo was shown in Fig. s2B, in which AuNPs were uniformly dispersed and the particle size was about 13 nm, which was consistent with the literature reports (Sun, Wang, Sun, Li, Song, Zhang, et al., 2020).

### 3.2. FRET between UCNPs and AuNPs

In this work, the UCNPs-AuNPs FRET system was constructed based on AuNPs induced UCNPs fluorescence quenching. FRET process was affected by three factors, the distance between the donor and the recipient, the spectral overlap of the donor and the receptor, and the relative orientation of the transition dipole (Jin, Wang, Lin, Jin, Zhang, Cui, et al., 2017). AuNPs generated by citric acid synthesis had negative charges and were uniformly stabilized in an aqueous solution due to the stronger electrostatic repulsion. Surface amination-modified UCNPs carried positive charges, so negatively charged AuNPs and positively charged UCNPs were close to each other through electrostatic interaction, resulting in FRET. As shown in Fig. 1A, the TEM photo of UCNPs@SiO<sub>2</sub>-NH<sub>2</sub>/AuNPs successfully verified the interaction. As shown in Fig. 1B, the absorption spectrum of AuNPs significantly overlapped with the emission spectrum of UCNPs, demonstrating that effective FRET could occur between UCNPs and AuNPs.

### 3.3. Principle of the FRET aptasensor for Amp

To verify the feasibility of this aptasensor for Amp detection, the effects of several related factors were investigated. UCNPs were incubated with Amp, NaCl, Apt, and Amp-Apt under the same conditions, respectively. As shown in Figure s3, their fluorescence intensities were as same as that of water-soluble UCNPs, so these factors can not affect the fluorescence of UCNPs.

The interactions of the components in the proposed Amp detection system are shown in Figure s4. UCNPs had a strong fluorescence signal at 540 nm. When mixed with AuNPs, the fluorescence intensity of UCNPs was significantly reduced, suggesting that FRET occurred between UCNPs and AuNPs. When AuNPs, NaCl, and UCNPs were mixed together, the fluorescence of UCNPs partially recovered, it was because the NaCl (salt) solution could shield the electrostatic repulsion between AuNPs, resulting in AuNPs aggregation, which greatly reduced the efficiency of FRET between UCNPs and AuNPs. When Apt, AuNPs, NaCl, and UCNPs were mixed together, UCNPs fluorescence was quenched again, the reason was that the Apt could be strongly adsorbed on the surface of AuNPs through the coordination between the nitrogen atoms (Apt) and AuNPs, enhancing the stability of AuNPs against the salt-induced aggregation (Chang, Chen, Wu, Yang, Lin, & Chen, 2019; Mondal, Ramlal, Lavu, & Kingston, 2018). When Amp, Apt, AuNPs, NaCl, and UCNPs were mixed, the fluorescence of UCNPs was restored again, its mechanism was that Apt and Amp were banded and Apt could not stabilize AuNPs, causing AuNPs to aggregate again. Therefore, the system of Apt, AuNPs, NaCl and UCNPs could be used for the detection

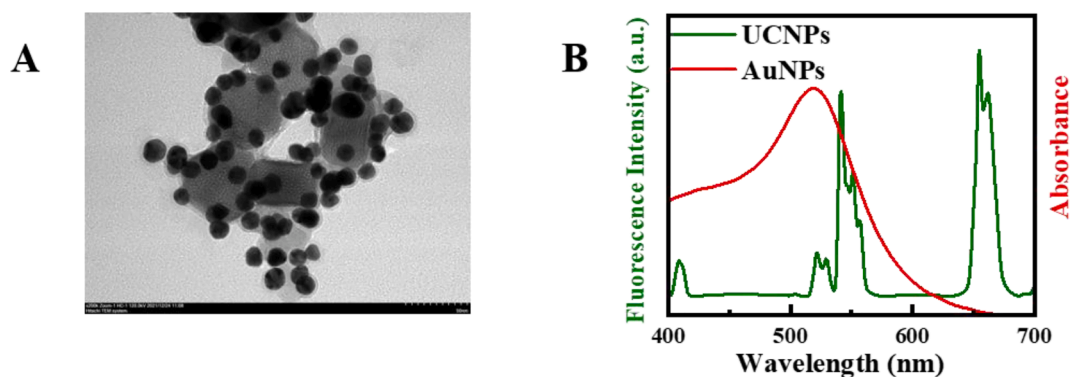


Fig. 1. TEM image of UCNPs/AuNPs (A) and their corresponding emission fluorescence/absorption spectra (B).

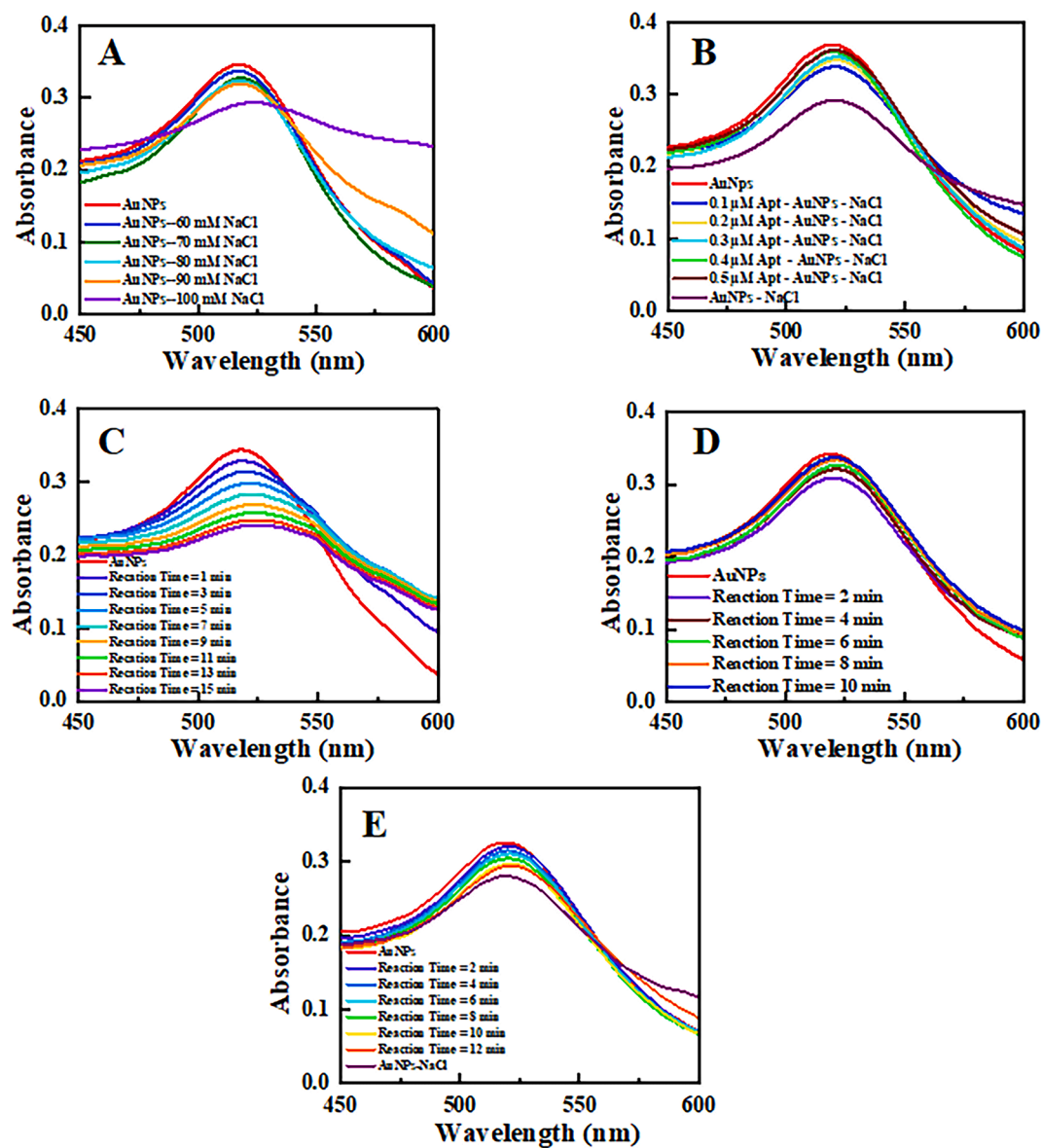


Fig. 2. Optimization of sodium chloride salt solution concentration (A), Apt concentration (B), and Optimization of reaction time of NaCl-AuNPs (C), Apt-AuNPs (D), and Apt-Amp(E).



of Amp.

### 3.4. Optimization of the detection conditions

To obtain a highly sensitive Amp sensor, several parameters, including NaCl and Apt concentrations, reaction time for NaCl-AuNPs, Apt-AuNPs, and Apt-Amp, were investigated, respectively.

The performance of the aptasensor largely depends on the number and distribution of donor (UCNPs) and receptor (AuNPs). NaCl concentration directly affected AuNPs aggregation, so it was necessary to optimize NaCl concentration. AuNPs were added to equal volume of NaCl solution (60, 70, 80, 90, 100 mM). After 10 min mixture, their absorption spectra were collected, and the results are shown in Fig. 2A. With the concentration increase of NaCl, the absorption peak at 520 nm of AuNPs decreased gradually, and its value tended to be stable at 90 mM NaCl, so the optimal NaCl concentration was 90 mM.

The Apt can be strongly adsorbed on the surface of AuNPs, improving the stability of AuNPs against the salt-induced aggregation, therefore, the concentration of Apt was also an important factor affecting their binding. Different concentrations (0.1, 0.2, 0.3, 0.4, 0.5  $\mu$ M) Apt were mixed with 4.8 nM AuNPs for 5 min, and 90 mM NaCl solution was added and mixed. 10 min later, the spectra of the solution were collected. The results are shown in Fig. 2B, with the increase of Apt concentration, the absorption value of AuNPs at 520 nm increased, which demonstrated that the protection of AuNPs aggregation in the salt solution was enhanced. When Apt concentration reached 0.4  $\mu$ M, the absorption value tended to be stable, therefore, 0.4  $\mu$ M Apt was selected for the aptasensor system.

In addition, the three reaction time, NaCl-AuNPs, Apt-AuNPs, and Apt-Amp, were optimized. Firstly, the time optimization for NaCl-AuNPs was investigated. As shown in Fig. 2C, with the reaction time of AuNPs and NaCl extended, the absorption peak of AuNPs at 520 nm gradually decreased, indicating that AuNPs aggregated. 13 min later, the absorption value tended to be stable, therefore, 13 min was the optimal reaction time. Secondly, the influence of reaction time on the binding of Apt and AuNPs was discussed. As shown in Fig. 2D, with the time increased, the absorption peak of AuNPs at 520 nm increased, indicating that the Apt's protection capability for AuNPs aggregation increased. When the reaction time was 8 min, Apt could be adsorbed on AuNPs well and the absorption value tended to be stable, therefore, 8 min was applied for the detection system. Finally, the specific binding time of Apt and Amp was optimized. As shown in Fig. 2E, with the increase of reaction time, the absorption peak of AuNPs at 520 nm decreased, indicating that AuNPs aggregated. When the reaction time was 10 min, the AuNPs absorption value tended to be stable, suggesting that Apt and Amp completed the specific recognition and binding, thus 10 min was applied in this detection system.

### 3.5. Amp detection

Fig. 3A shows the fluorescence spectra of the UCNPs/AuNPs/Apt/NaCl mixture under the presence of different concentrations of Amp ranging from 0 to 150 ng/mL. As shown in Fig. 3A, with the concentration of Amp increased, the fluorescence intensity at 540 nm of UCNPs gradually increased.

The plots of Amp concentration vs fluorescence intensity (540 nm) are shown in Fig. 3B. For 10–150 ng/mL Amp, the linear fitting equation was as follows:

$$y = 47.392x + 259.142 \quad (1)$$

where  $y$  and  $x$  represented fluorescence recovery and Amp concentration, and coefficient of determination ( $R^2$ ) was 0.9939, which demonstrated that they have a good linear relationship. The limit of detection (LOD) was calculated to be 3.9 ng/mL ( $S/N = 3$ ), which was lower than the safe level for milk (10  $\mu$ g/L). Thus, this aptasensor can quantitatively detect Amp at a low concentration.

A comparison of the different methods for Amp assay is summarized in Tab. s1. Compared with the HPLC and fluorescence colorimetry, the FRET aptasensor constructed in this work has a wide detection range. Although the sensitivity was lower than those of the HPLC and fluorescence colorimetry, its sensitivity was close to that of the ELISA method and better than that of the electrochemical method. Moreover, compared with others, the present method had the advantages of simple operation and potable, and it could meet the requirements of animal husbandry for the rapid detection of milk.

### 3.6. Specificity of the aptasensor for Amp

Selectivity is a very important parameter for the performance evaluation of a sensor. In this work, six antibiotics, including erythromycin, kanamycin, penicillin G, tetracycline, oxytetracycline, and azithromycin, were subjected to the same procedure as Amp detection. As shown in Fig. 4, only Amp caused significant fluorescence changes, while the changes caused by other antibiotics were small. It demonstrated that the designed fluorescent aptasensor has a high specificity for Amp detection.

### 3.7. Reproducibility and stability of the aptasensor for Amp

The stability and reproducibility of a sensor were of great significance for future practical applications. Three parallel measurements were performed on the samples containing 25 ng/mL Amp, the result showed that the relative standard deviation (RSD) was 3.49 %, which demonstrated that the aptasensor had good reproducibility. After the synthesized UCNPs were stored at 4 °C for one month, three parallel tests were performed on milk containing 25 ng/mL Amp, the test result showed that the absolute error of Amp was 2.28 ng/mL, and the RSD was

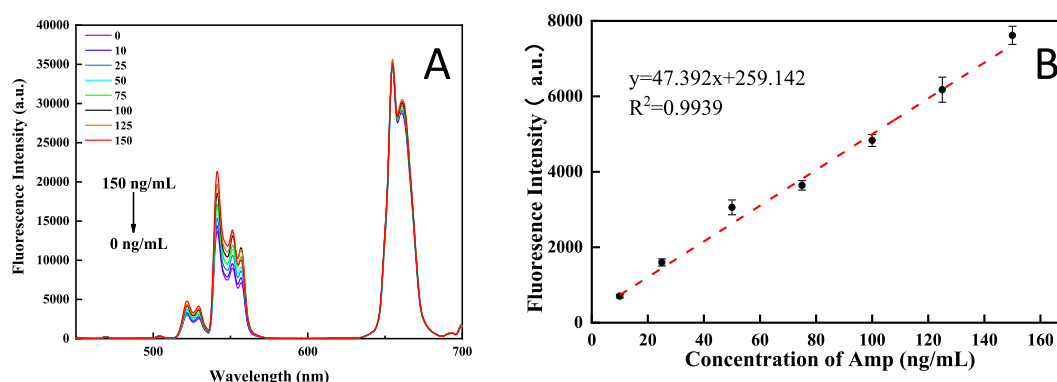


Fig. 3. Fluorescence emission spectra of UCNPs for detecting different concentrations of Amp, the original spectra (A), the regression fitting (B).

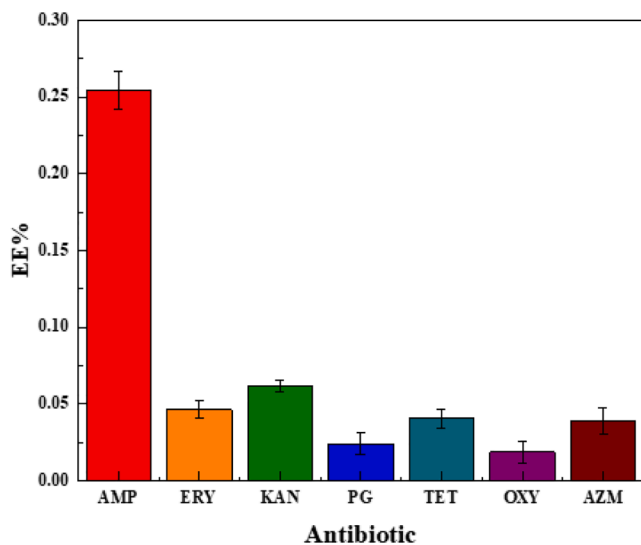


Fig. 4. Specificity assessment of upconversion fluorescence assays.

4.07 % (less than 5%), which demonstrated that this method had good stability for Amp detection.

### 3.8. Detection of Amp in milk samples

To investigate the applicability of the developed method for real sample determination, milk samples and Amp spiked milk samples were tested. According to the national standard method, the HPLC method was selected as the reference method. The results are shown in Table 1, for the milk sample, the Amp concentrations determined by the HPLC method and the developed method were N. D. and  $-0.95 \pm 0.88 \text{ ng mL}^{-1}$ , respectively, which demonstrated that this method worked well. For the 3 spiked milk samples, the recoveries of the 10  $\text{ng mL}^{-1}$ , 45  $\text{ng mL}^{-1}$ , and 100  $\text{ng mL}^{-1}$  spiked milk samples were 100.5 %, 101.2 % and 93.3 %, respectively, and the RSDs were 4.99 %, 5.80 % and 1.89 %, respectively. There were no statistical differences ( $p > 0.05$ ) between the reference method and the developed method, it suggested that there was no difference between the two detection methods.

The linear fitting equation for the results from the 2 methods was as follows:

$$y = 1.031x - 0.7917 \quad (2)$$

where  $y$  and  $x$  represented results from the HPLC and that from this method.  $R^2$  was 0.9944, it demonstrated that this method had a good relationship with the HPLC method. For this method, the average absolute error was  $2.04 \text{ ng mL}^{-1}$ , which was small; the average relative error was 4.2 %, which was lower than 5 %. Therefore, the developed aptasensor had a good detection performance, and can be used for the detection of Amp in milk sample.

Based on the wide detection range and simple operation, the proposed method had the advantages of low detection cost, rapidity, and easy portability. Regarding the limitation of this method, the LOD was relatively high compared to other methods (Tab. s1), however, it was suitable for the detection of Amp in milk.

## 4. Conclusion

This study successfully developed a novel aptasensor for Amp detection based on FRET between UCNPs and AuNPs. It can be used for the accurate determination of Amp in milk. Also, it had a potential capability for Amp detection in other samples. In addition, the proposed detection system can be easily applied for the detection of other targets by replacing suitable aptamers, it provided a new way for the

Table 1

Comparison of the determination results for milk samples by the reference method and the developed method.

Samples	Spiked (ng mL <sup>-1</sup> )	HPLC method (ng·mL <sup>-1</sup> )	This method (ng·mL <sup>-1</sup> )	Recovery (%)	RSD <sup>b</sup> (%)	$p^c$
1	0	N. D. <sup>a</sup>	$-0.95 \pm 0.88$	–	–	–
2	10	$9.26 \pm 0.38$	$10.05 \pm 0.50$	100.5	4.99	0.15
3	45	$47.44 \pm 1.42$	$45.53 \pm 2.64$	101.2	5.80	0.42
4	100	$90.02 \pm 3.19$	$93.33 \pm 1.77$	93.3	1.89	0.27

<sup>a</sup> N. D.: not detect.

<sup>b</sup> RSD:(standard deviation)/mean  $\times 100$  %,  $n = 3$ .

<sup>c</sup>  $p > 0.05$ , indicate: no significant difference.

applications in agriculture, environment, and biomedical areas.

## Funding

This work was supported by the Jiangsu Provincial Key Research and Development Program (No. BE2020331) and the National Modern Agricultural Industry Technology System Project (No. CARS-18).

## CRedit authorship contribution statement

**Chong Chen:** Methodology, Validation, Formal analysis, Data curation, Writing – original draft. **Hong Lei:** Investigation, Methodology. **Nan Liu:** Investigation, Methodology. **Hui Yan:** Conceptualization, Resources, Data curation, Writing – review & editing, Supervision, Funding acquisition.

## Declaration of Competing Interest

The authors declare that they have no known competing financial interests or personal relationships that could have appeared to influence the work reported in this paper.

## Appendix A. Supplementary data

Supplementary data to this article can be found online at <https://doi.org/10.1016/j.fochx.2022.100439>.

## References

- Abouzied, M., Sarzynski, M., Walsh, A., Wood, H., & Mozola, M. (2009). Validation study of a receptor-based lateral flow assay for detection of beta-lactam antibiotics in milk. *Journal of AOAC International*, 92(3), 959–974.
- Chang, C.-C., Chen, C.-P., Wu, T.-H., Yang, C.-H., Lin, C.-W., & Chen, C.-Y. (2019). Gold nanoparticle-based colorimetric strategies for chemical and biological sensing applications. *Nanomaterials*, 9(6), 861.
- Chen, Q., Sheng, R., Wang, P., Ouyang, Q., Wang, A., Ali, S., ... Hassan, M. M. (2020). Ultra-sensitive detection of malathion residues using FRET-based upconversion fluorescence sensor in food. *Spectrochimica Acta Part A: Molecular and Biomolecular Spectroscopy*, 241, Article 118654.
- Cheng, P.-C. (2006). *The contrast formation in optical microscopy*. In *Handbook of biological confocal microscopy* (pp. 162–206). Springer.
- Elmolla, E. S., & Chaudhuri, M. (2011). The feasibility of using combined TiO<sub>2</sub> photocatalysis-SBR process for antibiotic wastewater treatment. *Desalination*, 272(1–3), 218–224.
- FitzGerald, S. P., O'Loan, N., McConnell, R. I., Benchikh, E. O., & Kane, N. E. (2007). Stable competitive enzyme-linked immunosorbent assay kit for rapid measurement of 11 active beta-lactams in milk, tissue, urine, and serum. *Journal of AOAC International*, 90(1), 334–342.
- Frens, G. (1973). Controlled nucleation for the regulation of the particle size in monodisperse gold suspensions. *Nature physical science*, 241(105), 20–22.
- Gan, Z., Hu, X., Xu, X., Zhang, W., Zou, X., Shi, J., ... Arslan, M. (2021). A portable test strip based on fluorescent europium-based metal-organic framework for rapid and visual detection of tetracycline in food samples. *Food Chemistry*, 354, Article 129501.
- Gao, C., Zheng, P., Liu, Q., Han, S., Li, D., Luo, S., ... Wei, Y. (2021). Recent Advances of Upconversion Nanomaterials in the Biological Field. *Nanomaterials*, 11(10), 2474.

- Guo, S., Xie, X., Huang, L., & Huang, W. (2016). Sensitive water probing through nonlinear photon upconversion of lanthanide-doped nanoparticles. *ACS Applied Materials & Interfaces*, 8(1), 847–853.
- Haiss, W., Thanh, N. T., Aveyard, J., & Fernig, D. G. (2007). Determination of size and concentration of gold nanoparticles from UV-Vis spectra. *Analytical Chemistry*, 79(11), 4215–4221.
- Helms, V. (2008). *Fluorescence Resonance Energy Transfer*. In *Principles of Computational Cell Biology* (p. pp. 202). Weinheim: Wiley-VCH.
- Jalil, R. A., & Zhang, Y. (2008). Biocompatibility of silica coated NaYF<sub>4</sub> upconversion fluorescent nanocrystals. *Biomaterials*, 29(30), 4122–4128.
- Jin, B., Wang, S., Lin, M., Jin, Y., Zhang, S., Cui, X., ... Lu, T. J. (2017). Upconversion nanoparticles based FRET aptasensor for rapid and ultrasensitive bacteria detection. *Biosensors and Bioelectronics*, 90, 525–533.
- Li, F., Zhu, J., Li, R., Liu, Y., Li, Z., & Kang, H. (2020). Magnetic bead-based electrochemical aptasensor doped with multi-wall carbon nanotubes for the detection of ampicillin in milk. *International Journal of Electrochemical Science*, 15, 7520–7530.
- Li, H., Wang, X., Huang, D., & Chen, G. (2019). Recent advances of lanthanide-doped upconversion nanoparticles for biological applications. *Nanotechnology*, 31(7), Article 072001.
- Lin, B., Yu, Y., Cao, Y., Guo, M., Zhu, D., Dai, J., & Zheng, M. (2018). Point-of-care testing for streptomycin based on aptamer recognizing and digital image colorimetry by smartphone. *Biosensors and Bioelectronics*, 100, 482–489.
- Liu, Y., Ouyang, Q., Li, H., Zhang, Z., & Chen, Q. (2017). Development of an inner filter effects-based upconversion nanoparticles–curcumin nanosystem for the sensitive sensing of fluoride ion. *ACS Applied Materials & Interfaces*, 9(21), 18314–18321.
- Long, Q., Li, H., Zhang, Y., & Yao, S. (2015). Upconversion nanoparticle-based fluorescence resonance energy transfer assay for organophosphorus pesticides. *Biosensors and Bioelectronics*, 68, 168–174.
- Luo, W., Ang, C. Y., & Thompson, H. C., Jr (1997). Rapid method for the determination of ampicillin residues in animal muscle tissues by high-performance liquid chromatography with fluorescence detection. *Journal of Chromatography B: Biomedical Sciences and Applications*, 694(2), 401–407.
- Mondal, B., Ramlal, S., Lavu, P. S., & Kingston, J. (2018). Highly sensitive colorimetric biosensor for Staphylococcal enterotoxin B by a label-free aptamer and gold nanoparticles. *Frontiers in microbiology*, 9, 179.
- Shi, H., Zhao, G., Liu, M., Fan, L., & Cao, T. (2013). Aptamer-based colorimetric sensing of acetamiprid in soil samples: Sensitivity, selectivity and mechanism. *Journal of hazardous materials*, 260, 754–761.
- Song, K.-M., Jeong, E., Jeon, W., Cho, M., & Ban, C. (2012). Aptasensor for ampicillin using gold nanoparticle based dual fluorescence–colorimetric methods. *Analytical and Bioanalytical Chemistry*, 402(6), 2153–2161.
- Sun, L., Wang, T., Sun, Y., Li, Z., Song, H., Zhang, B., ... Hu, J. (2020). Fluorescence resonance energy transfer between NH<sub>2</sub>-NaYF<sub>4</sub>: Yb, Er/NaYF<sub>4</sub>@ SiO<sub>2</sub> upconversion nanoparticles and gold nanoparticles for the detection of glutathione and cadmium ions. *Talanta*, 207, Article 120294.
- Wang, M., Hou, W., Mi, C.-C., Wang, W.-X., Xu, Z.-R., Teng, H.-H., ... Xu, S.-K. (2009). Immunoassay of goat antihuman immunoglobulin G antibody based on luminescence resonance energy transfer between near-infrared responsive NaYF<sub>4</sub>: Yb, Er upconversion fluorescent nanoparticles and gold nanoparticles. *Analytical Chemistry*, 81(21), 8783–8789.
- Wu, S., Duan, N., Ma, X., Xia, Y., Wang, H., Wang, Z., & Zhang, Q. (2012). Multiplexed fluorescence resonance energy transfer aptasensor between upconversion nanoparticles and graphene oxide for the simultaneous determination of mycotoxins. *Analytical Chemistry*, 84(14), 6263–6270.
- Xu, W., Chen, X., & Song, H. (2017). Upconversion manipulation by local electromagnetic field. *Nano Today*, 17, 54–78.
- Yang, C., Li, Y., Wu, N., Zhang, Y., Feng, W., Yu, M., & Li, Z. (2021). Ratiometric upconversion luminescence nanoprobe for quick sensing of Hg<sup>2+</sup> and cells imaging. *Sensors and Actuators B: Chemical*, 326, Article 128841.
- Zong, L., Jiao, Y., Guo, X., Zhu, C., Gao, L., Han, Y., ... Liu, J. (2019). based fluorescent immunoassay for highly sensitive and selective detection of norfloxacin in milk at picogram level. *Talanta*, 195, 333–338.